

Variational calculations of the excited states of liquid <sup>4</sup>He

K. E. Schmidt\* and V. R. Pandharipande

Department of Physics, University of Illinois at Urbana-Champaign, Illinois 61801

(Received 9 October 1979)

Approximate wave functions of the form  $\mathcal{G}\Phi(n(\vec{k}))$ , where  $\mathcal{G}$  is a correlation operator that contains two-body, three-body, and momentum-dependent correlations, and  $\Phi(n(\vec{k}))$  is a noninteracting-Bose-gas wave function with occupation numbers  $n(\vec{k})$ , are used to calculate the energies of excited states of liquid <sup>4</sup>He. The energy expectation values are calculated by generalizing the Fermi hypernetted-chain methods. The single-quasiparticle excitation spectrum provides stringent tests for the correlation operator  $\mathcal{G}$ . The calculated phonon, maxon spectra are not in good agreement with the experimental results presumably because of the truncations in the large-distance behavior of the two-body correlations in the  $\mathcal{G}$ . The results obtained for the roton energies are in good agreement with the experiments over the range of liquid-<sup>4</sup>He density.

I. INTRODUCTION

A one-to-one correspondence between the low-lying states of interacting and noninteracting quantum fluids is implicit in Landau's quasiparticle approach to the theory of quantum fluids. This correspondence implies the existence of a correlation operator  $\mathcal{G}$  that transforms the noninteracting states  $\Phi_i$  into interacting states  $\Psi_i$ :

$$\Psi_i(n_i(\vec{k})) = \mathcal{G}\Phi_i(n_i(\vec{k})) \quad (1.1)$$

The noninteracting states are specified by the occupation numbers  $n_i(\vec{k})$  of the single-particle states, and the correspondence allows also the  $\Psi_i$  to be labeled with the  $n_i(\vec{k})$ .

Let  $n_0(\vec{k})$  be the occupation numbers in the ground state. The difference  $\delta_i(\vec{k})$ ,

$$\delta_i(\vec{k}) = n_i(\vec{k}) - n_0(\vec{k}) \quad (1.2)$$

specifies the quasiparticle excitations in the state  $\Psi_i$ . In Bose liquids the states  $\Psi_{\vec{k}}(n_{\vec{k}}(\vec{k}))$ ,

$$\delta_{\vec{k}}(\vec{k} = \vec{K}) = 1 \quad ,$$

$$\delta_{\vec{k}}(k = 0) = -1 \quad ,$$

$$\delta_{\vec{k}}(\vec{k} \neq 0 \text{ or } \vec{K}) = 0 \quad ,$$

which correspond to the  $\Phi_{\vec{k}}$  given by

$$\Phi_{\vec{k}}(n_{\vec{k}}(\vec{k})) = \sum_i \exp(i\vec{K} \cdot \vec{r}_i) \quad , \quad (1.3)$$

are identified with the phonon-roton excitations of momentum  $\vec{K}$ . In their pioneering calculation of the phonon-roton spectrum in liquid <sup>4</sup>He, Feynman and Cohen<sup>1</sup> (FC) used the correlation operator

$$\mathcal{G}_{FC} = \hat{\Psi}_0 \left[ 1 + \sum_{i < j} \beta_k \frac{1}{r_{ij}^3} \vec{r}_{ij} \cdot \vec{\nabla}_{ij} \right] \quad , \quad (1.4)$$

where  $\hat{\Psi}_0$  is the exact ground-state wave function, to

generate the approximate  $\Psi_{\vec{k}}$ . We emphasize exact wave functions and energies with a caret. FC did not attempt to calculate either the  $\hat{\Psi}_0$  or  $\hat{E}_0$ . They developed their theory specifically to explain the excitation spectrum of liquid <sup>4</sup>He using the experimentally known static structure function.

Recently<sup>2,3</sup> an improved description of the ground state  $\Psi_0$  of both liquid <sup>4</sup>He and <sup>3</sup>He has been obtained with the correlation operator

$$\mathcal{G} = \prod_{i < j} f_{J,ij} \prod_{i < j < k} f_{3,ijk} \prod_{i < j} f_{K,ij} \quad . \quad (1.5)$$

The  $f_{J,ij}$  is a two-body Jastrow correlation function of  $|\vec{r}_i - \vec{r}_j|$ , while

$$f_{K,ij} = 1 + \frac{\eta_{ij}}{f_{J,ij}} \vec{r}_{ij} \cdot \vec{\nabla}_{ij}^R \quad (1.6)$$

incorporates the FC backflow, and the  $\vec{\nabla}_{ij}^R$  are restricted to operate on the  $\Phi$ . The three-body correlation  $f_{3,ijk}$  contains terms of type  $\eta_{ij} \vec{r}_{ij} \cdot (\nabla_i f_{J,ik})$ , and it is in principle determined by the two-body functions  $f_{J,ij}$  and  $\eta_{ij}$ . The approximations in this  $\mathcal{G}$ , and the calculation of  $f_{J,ij}$ ,  $\eta_{ij}$ , and  $f_{3,ijk}$  are discussed in Refs. 2 and 3 which we henceforth denote by I and II, respectively.

Fermi hypernetted-chain summation methods are used in II to calculate expectation values with the wave functions  $\mathcal{G}\Phi_i$  in Fermi liquids. In Secs. II and IV these methods are further developed to calculate the  $E(n(\vec{k}))$  of the excited states of Bose liquids. The theory is developed for an arbitrary  $n(\vec{k})$  with the hope that it will be useful in extending the variational method proposed for Fermi liquids at finite temperatures<sup>4</sup> to Bose liquids.

We calculate  $\langle \Psi_i | H | \Psi_i \rangle / \langle \Psi_i | \Psi_i \rangle$  directly, where as in past<sup>5-7</sup> the excitation spectrum has been obtained by calculating  $\langle \Psi_{\vec{k}} | H | \Psi_{\vec{k}} \rangle / \langle \Psi_0 | \Psi_0 \rangle$  and  $\langle \Psi_{\vec{k}} | \Psi_{\vec{k}} \rangle / \langle \Psi_0 | \Psi_0 \rangle$  separately. When  $\mathcal{G}$  does not contain any backflow correlation the  $\langle \Psi_{\vec{k}} | \Psi_{\vec{k}} \rangle / \langle \Psi_0 | \Psi_0 \rangle$  for the one-quasiparticle excitations be-

comes simply  $\mathcal{S}(\bar{\mathbf{K}})$  the liquid structure function. We expect our formalism will be convenient for an arbitrary  $\Psi_i(n_i(\bar{\mathbf{K}}))$ .

The cluster expansion for Bose  $E(n(\bar{\mathbf{k}}))$  is quite similar to that of the Fermi  $E(n(\bar{\mathbf{k}}))$ , except for extra exchange loops that are needed to describe the exchange of particles in  $\bar{\mathbf{k}} \neq 0$  states with those in the  $\bar{\mathbf{k}} = 0$  condensate. When  $n(\bar{\mathbf{k}} \neq 0) = 0$  the cluster expansion reduces to that of  $E_0$  discussed in I, and it has no exchange loops. We emphasize that the  $n(\bar{\mathbf{k}})$  refer to occupations in  $\Phi$ , so  $n(\bar{\mathbf{k}} \neq 0) = 0$  does not imply that all the particles in  $\Psi_0$  are in the condensate.

In Sec. V we calculate the  $E(n_{\bar{\mathbf{k}}}(k))$ , and thus the phonon-rotor spectrum in liquid  ${}^4\text{He}$ , using the de-Boer and Michels<sup>8</sup> Lennard-Jones potential (in K)

$$v(r) = 40.88 \left[ \left( \frac{\sigma}{r} \right)^{12} - \left( \frac{\sigma}{r} \right)^6 \right], \quad (1.7)$$

$$\sigma = 2.556 \text{ \AA}, \quad (1.8)$$

and the  $\mathcal{G}$  given by Eq. (1.5). The calculations are carried out at various densities. Our object is to develop a consistent microscopic theory of the ground and excited states of liquid  ${}^4\text{He}$ , and thus our calculations differ from the FC calculations in the following respects.

Microscopically we do not know the exact correlation operator  $\hat{\mathcal{G}}$  that will give the  $\hat{\Psi}_0$ . The  $\Psi_0$  given by the  $\mathcal{G}$  is

$$\Psi_0 = \prod_{i < j} f_{j,ij} \prod_{i < j < k} f_{3,ijk}, \quad (1.9)$$

and we can express the  $\mathcal{G}$  in FC form as

$$\mathcal{G} = \Psi_0 \prod_{i < j} f_{k,ij}. \quad (1.10)$$

The  $E(n(\bar{\mathbf{k}}))$  contains a contribution

$$\frac{\langle \Phi(n(\bar{\mathbf{k}})) | \mathcal{G}^\dagger (H \Psi_0) \prod_{i < k} f_{k,ij} | \Phi(n(\bar{\mathbf{k}})) \rangle}{\langle \Phi(n(\bar{\mathbf{k}})) | \mathcal{G}^\dagger \mathcal{G} | \Phi(n(\bar{\mathbf{k}})) \rangle}, \quad (1.11)$$

which includes the entire potential energy, and the kinetic-energy terms in which the  $\nabla_i^2$  operators operate on the  $\Psi_0$ . This contribution is given by the sum of the terms  $W$ ,  $U$ , and  $T$  of Sec. V. FC did not need to calculate this contribution; for the exact  $\hat{\Psi}_0$

$$H \hat{\Psi}_0 = \hat{E}_0 \hat{\Psi}_0 \quad (1.12)$$

and the above contribution is  $\hat{E}_0$ . We must calculate it because the approximate  $\Psi_0$  need not satisfy Eq. (1.12). It is found that, particularly due to the  $f_{3,ijk}$  in the  $\Psi_0$ , this contribution to  $E(n_{\bar{\mathbf{k}}}(\bar{\mathbf{K}}))$  is indeed very close to  $E_0$  over a wide range of  $\bar{\mathbf{K}}$ , except at very small  $\bar{\mathbf{K}}$ .

Since we work with a known  $\Psi_0$  we can in principle avoid the approximations that FC make for the many-particle distribution functions that are not experimentally measured. In practice, however, some approximations are necessary in computing the distribution functions from the  $\Psi_0$ , unless a Monte Carlo simulation<sup>6</sup> is carried out on a computer.

The excitation spectrum offers a more stringent test of the  $\mathcal{G}$  than the ground-state energy. For example the long-range  $r^{-2}$  component of  $f_{j,ij}$  has a small effect on the  $E_0$ , but our failure to obtain the correct small- $\bar{\mathbf{K}}$  part of the spectrum can be attributed to the absence of this component in our  $\mathcal{G}$ . The computed maxon energies are much too high, and this is probably due to the missing  $1/r_{ij}^3$  tail of the  $\eta_{ij}$ . The roton energies are in reasonable agreement with the experiment over a wide density range.

## II. CLUSTER EXPANSION

To begin with, we develop a diagrammatic cluster expansion to calculate expectation values with the simpler wave function

$$\Psi_s(n(\bar{\mathbf{k}})) = \prod_{i < j} f_{j,ij} \prod_{i < j < k} f_{3,ijk} \mathcal{S} \left[ \prod_i \exp[i \bar{\mathbf{k}}(i) \cdot \bar{\mathbf{r}}_i] \right], \quad (2.1)$$

$$\bar{\mathbf{k}}(1) = \bar{\mathbf{k}}(2) = \dots = \bar{\mathbf{k}}(n(0)) = 0, \quad (2.2)$$

$$\bar{\mathbf{k}}(n(0) + 1) = \bar{\mathbf{k}}(n(0) + 2) = \dots = \bar{\mathbf{k}}(n(0) + n(\bar{\mathbf{k}}_1)) = \bar{\mathbf{k}}_1 \dots \quad (2.2)$$

The  $\mathcal{S}$  is a symmetrizing operator. We will assume that  $n(0)$  can be large and approach  $\infty$  in the limit the volume  $\Omega \rightarrow \infty$ , but all  $n(\bar{\mathbf{k}} \neq 0)$  are finite, and define a quasicondensate fraction  $p$  as

$$p = \frac{n(0)}{A}, \quad (2.3)$$

where  $A$  is the total number of atoms

$$A/\Omega = \rho. \quad (2.4)$$

A diagrammatic cluster expansion for the expectation value of a two-body operator  $\Theta(r)$

$$\frac{\int \left[ S \prod_i \exp[-i\vec{k}(i) \cdot \vec{r}_i] \prod_{i < j} f_{J,ij} \prod_{i < j < k} f_{3,ijk} \Theta_{mn}(r_{mn}) \prod_{i < j < k} f_{3,ijk} \prod_{i < j} f_{J,ij} \prod_i \exp[i\vec{k}(i) \cdot \vec{r}_i] d\tau \right]}{\int \left[ S \prod_i \exp[-i\vec{k}(i) \cdot \vec{r}_i] \prod_{i < j} f_{J,ij}^2 \prod_{i < j < k} f_{3,ijk}^2 \prod_i \exp[i\vec{k}(i) \cdot \vec{r}_i] d\tau \right]} \quad (2.5)$$

is obtained, as in II, by replacing all the  $f_{J,ij}^2$ , except  $f_{J,mn}^2$  in the numerator, by  $1 + F$ , and all the  $f_3$  by  $1 + \sum_{\text{cyc}} \chi_{ijk}$ . For our choice of  $f_3$

$$\chi_{ijk} = \beta_3^2 \frac{\eta_{ij}\eta_{ik}}{f_{J,ij}f_{J,ik}} \bar{r}_{ij} \cdot \bar{r}_{ik} \quad (2.6)$$

where  $\beta_3$  is a variational parameter. The various integrals in the expansion of the numerator and the denominator are then represented by diagrams in which the points represent the particle coordinates,  $F_{ij}$  is a dashed line joining  $i$  and  $j$ , and solid lines  $ij$  and  $ik$  with a marking on the angle  $i$  of the triangle  $ijk$  denote  $\chi_{ijk}$ . All numerator diagrams must contain the points  $m$  and  $n$  and the function  $f_{mn} \Theta_{mn} f_{mn}$ .

Exchanges are represented by directed lines. An exchange line labeled  $\vec{k}(i)$  going from  $i$  to  $j$  represents the contribution of a term in  $\Psi^*$  in which particle  $j$  occupies the state  $\vec{k}(i)$ . We symmetrize only the left-hand  $\Psi^*$  and thus particles  $i, j, \dots$ , respectively, occupy states  $\vec{k}(i), \vec{k}(j), \dots$ , in the right-hand  $\Psi$ . All exchange lines  $\vec{k}(i)$  must thus originate from the point  $i$ . Exchange lines having  $\vec{k} \neq 0$  are called  $l$  lines; their rules are similar to those of exchange lines in Fermi liquids.<sup>3</sup> Exchange lines having  $k = 0$  are called  $p$  lines; they are dashed while the  $l$  lines are solid, and their diagram rules are discussed below.

In diagram 1.1 (of Fig. 1) we show a diagram with an exchange loop made up of two  $p$  lines. This diagram is not allowed since it represents a term in which both particles 1 and 2 are in the quasicondensate in  $\Psi^*$ . This term has already been counted by the direct diagram 1.2. Similarly diagrams, such as 1.3, having exchange loops with two  $p$  lines depict exchanges which have already been counted by diagrams, such as 1.4, which contain only one  $p$  line per exchange loop. These restrictions can be incorporated in a single diagram rule which states that all permissible exchange loops can be formed with any number of  $l$  lines and at most one  $p$  line. For convenience we will refer to an exchange loop as an  $l$  loop if it is made up of only  $l$  lines, and as a  $p$  loop if it contains a  $p$  line. Lastly we note that diagrams such as 1.5 and 1.6 in which uncorrelated particles are exchanged give zero contribution due to the

orthogonality of plane waves, and they should be discarded.

Diagrams depicting expectation values with Fermi liquid wave functions do not have  $p$  loops. In absence of  $f_K$  the cluster expansion for Fermi systems is irreducible; i.e., the reducible numerator diagrams cancel the denominator and the expectation value equals the sum of irreducible numerator diagrams. However, the restrictions on the  $p$  lines spoil this cancellation of the denominator in Bose systems. Therefore, the cluster expansion for expectation values with excited Bose liquid wave functions is not irreducible. Expectation values with the Bose ground state  $\Psi_0$  have no exchange diagrams and are thus given by the sum of irreducible numerator diagrams.

We use the general cluster expansion for an expectation value given by Wiringa and Pandharipande.<sup>9</sup>

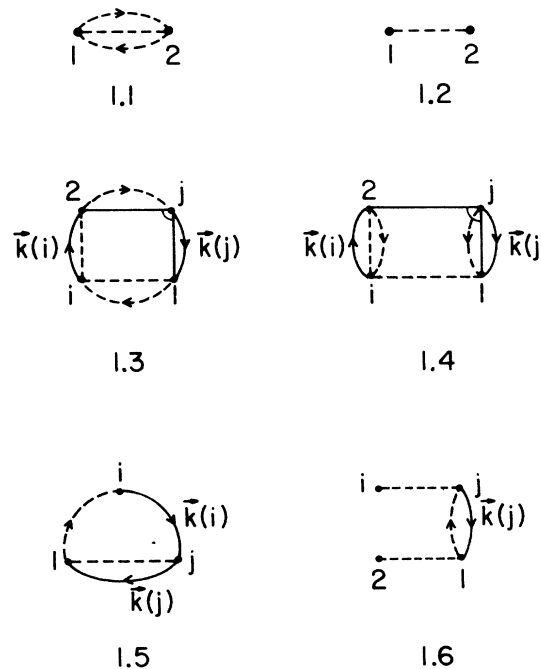


FIG. 1. Examples of diagrams having  $p$  exchange loops.

They give the following result:

$$\langle 0 \rangle = [A] + \{[\overline{Aa}] - [\overline{A}][\overline{a}]\} + \{[\overline{Aab}] - [\overline{Aa}][\overline{b}] - [\overline{A}][\overline{ab}] + [\overline{A}][\overline{a}][\overline{b}]\} + \{ \frac{1}{2}[\overline{Aab}] - [\overline{Aa}][\overline{b}] + \frac{1}{2}[\overline{A}][\overline{a}][\overline{b}] \} + \{ \frac{1}{2}[\overline{Aab}] - [\overline{Aa}][\overline{b}] - \frac{1}{2}[\overline{A}][\overline{ab}] + [\overline{A}][\overline{a}][\overline{b}] \} + \dots \quad (2.7)$$

where . . . represent terms having  $\geq 4$  inseparable pieces. The notation in the above expression is as follows:

(i)  $A, a, b, \dots$ , denote irreducible diagrams that cannot be broken into two pieces by cutting them at one point. The capital  $A$  represents elements of the set of the numerator diagrams that contain the operator  $\mathcal{O}_{mn}$ , while the lower case letters  $a, b, \dots$  denote diagrams that do not contain  $\mathcal{O}_{mn}$ . These could come from either the numerator or denominator.

(ii) Overhead lines denote common particle labels, for example  $\overline{Aa}$  indicates that the elements  $A$  and  $a$  have a common particle label. Two overhead lines  $\overline{Aab}$  denote that  $A$  and  $a$  have one common particle label, while  $a$  and  $b$  have another common particle label. A single common particle label in  $A$ ,  $a$ , and  $b$  is denoted by  $\overline{Aab}$ .

(iii) Connected diagrams are enclosed in  $[ ]$ . Thus  $[\overline{Aa}]$  denotes a connected reducible numerator diagram whose articulation point is the common particle, while  $[\overline{Aab}]$  is a reducible diagram with two articulation points. Terms having two or more  $[ ]$ 's denote products of disconnected diagrams.  $[A][a]$  for example denotes the product of  $[A]$  and  $[a]$ .

(iv) A summation over all elements  $A, a, b, \dots$ , of the sets of irreducible diagrams is implied with the restriction that the elements  $A, a, b$  of a given term, such as  $[\overline{Aa}][\overline{b}]$ , satisfy all common particle relationships specified by the overhead lines.

Normally terms enclosed in curly brackets of Eq. (2.7) cancel each other and only the sum of irreducible diagrams  $[A]$  survives. However, this cancellation does not necessarily occur for terms in which  $A, a, \dots$ , have  $p$  loops passing through the point having the common particle label. We can restrict our analysis to these terms only.

The simplest element in the set  $A$  containing a  $p$  loop is shown in diagram 2.1 (of Fig. 2), while the simplest element of this type in set  $a$  is diagram 2.2 of Fig. 2. Let us pretend for simplicity that the sets  $A$  and  $a$  have only elements of type 2.1 and 2.2, respectively. The sum over  $A, a, b, \dots$ , etc., will then become that over particle label of diagrams 2.1 and 2.2. Note that  $m > n(0)$ ,  $i > n(0)$  because there is an  $l$  line that starts from these vertices, and similarly  $n < n(0)$  and  $j < n(0)$ .

The  $[\overline{A}][\overline{a}]$  terms that can be constructed with these simplified sets are shown in diagrams 2.3 and 2.4. The diagram 2.5 is an  $[\overline{Aa}]$  term because the

exchange line  $ni$  can be "bent" to make it go from  $n$  to  $m$  and  $m$  to  $i$ , and it cancels the  $[\overline{A}][\overline{a}]$  term 2.3. However, there is no  $[\overline{Aa}]$  term that will cancel the  $[\overline{A}][\overline{a}]$  contribution 2.4. The  $[\overline{Aa}]$  diagram required to cancel 2.4 is shown in diagram 2.6; it has two  $p$  lines in a loop and thus does not exist.

We can similarly analyze the terms in Eq. (2.7) that have three separable pieces. Within the simplified set of diagrams we find that only the term  $[\overline{A}][\overline{a}][\overline{b}]$  shown in diagram 2.7 is left uncanceled. The uncanceled terms 2.1, 2.4, 2.7, and higher terms having  $\geq 4$  pieces that contain the element 2.1 of the set  $A$ , form a geometric series which can be summed to all orders. The sum is illustrated in diagram 2.8.

We can think of the coefficient of diagram 2.1 in

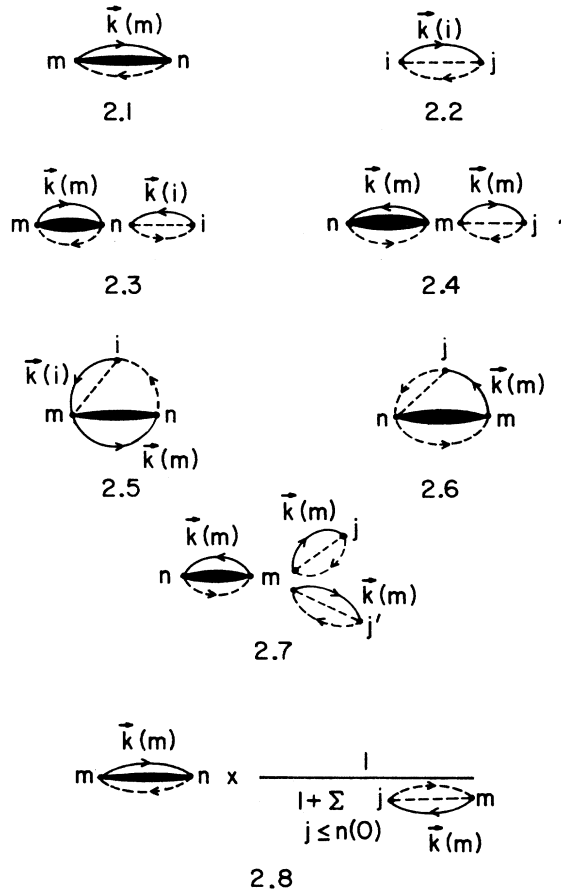
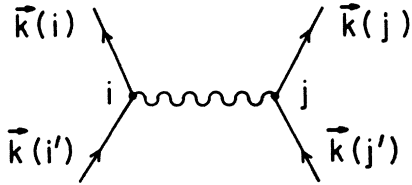


FIG. 2. Exchange diagrams that give vertex corrections.

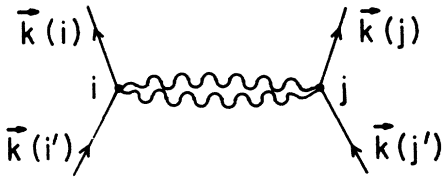
diagram 2.8 as a correction to the vertex  $m$  of 2.1. All other reducible contributions can also be included as corrections at the vertex  $m$  of the irreducible diagram 2.1. All the elements of the full set  $A$  that have a  $p$  loop containing an  $l$  line labeled  $\bar{k}(m)$  starting from  $m$  will contribute to this correction, and if we define their sum to be  $\hat{S}(\bar{k}(m)) - 1$  the vertex correction will be  $\hat{S}(\bar{k}(m))^{-1}$ .

Since the vertex correction depends on  $\bar{k}(m)$  it is more convenient to associate it with the  $l$  line labeled  $\bar{k}(m)$  starting from the vertex  $m$ . It may be verified that when we multiply all  $l$  lines, labeled  $\bar{k}(i)$ , in all  $p$  loops by  $\hat{S}(\bar{k}(i))^{-1}$ , all the reducible diagrams are automatically summed when diagrams of the irreducible set  $A$  are summed.

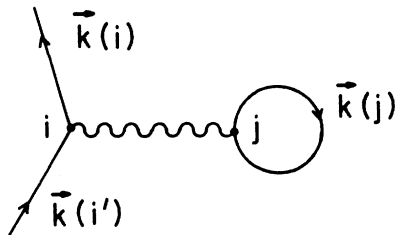
We may now sum over the particle labels of topologically identical diagrams. Apart from trivial symmetry factors we get a factor  $\rho$  at each vertex, and all exchange lines  $ij$  become simple functions of  $r_{ij}$ . The



3.1



3.2



3.3

FIG. 3. Diagrammatic elements depicting  $(f_{k,ij} - 1)$ .

$l$  lines in  $l$  loops become  $l_{ij}$ ,

$$l_{ij} = \frac{1}{A} \sum_{k>0} \exp(i\bar{k} \cdot \bar{r}_{ij}) n(\bar{k}) \quad (2.8)$$

while the  $l$  lines in  $p$  loops give  $\hat{l}_{ij}$

$$\hat{l}_{ij} = \frac{1}{A} \sum_{k>0} \frac{\exp(i\bar{k} \cdot \bar{r}_{ij})}{\hat{S}(\bar{k})} n(\bar{k}) \quad (2.9)$$

and the  $p$  line gives the factor  $p$ .

Expectation values with the full wave function  $\Psi(n(\bar{k}))$ , which contains the  $f_K$  correlation have additional diagrams that represent the contribution of terms in the expansion of  $(\prod_{i<j} f_{K,ij} - 1)$ . The  $f_{K,ij} - 1$  is represented by a wavy line joining  $i$  and  $j$ , its contribution depends on the states occupied by  $i$  and  $j$ . The single wavy line shown in diagram 3.1 (of Fig. 3) gives

$$\frac{1}{2} i f_{j,ij} \eta_{ij} \bar{r}_{ij} \cdot [\bar{k}(i) - \bar{k}(j) - \bar{k}(i') + \bar{k}(j')] \quad ,$$

while the double wavy line of diagram 3.2 gives

$$-\frac{1}{4} \eta_{ij}^2 \bar{r}_{ij} \cdot [\bar{k}(j') - \bar{k}(i')] \bar{r}_{ij} \cdot [\bar{k}(i) - \bar{k}(j)] \quad .$$

In dealing with wavy-line diagrams it is useful to imagine a closed directed loop labeled  $\bar{k}(j)$ , illustrated in diagram 3.3, at every direct vertex  $j$ . Note that a single wavy line connecting two direct vertices gives zero contribution. Diagrams containing wavy lines in exchange loops are often not reducible, because to reduce exchange diagrams (2.5 for example), we often have to "bend" exchange lines, and this changes the  $f_K$  contribution. These diagrams have to be treated with the general expansion (2.7), as is done in II.

### III. CHAIN SUMMATIONS

The hypernetted-chain (HNC) integral equations for Bose excited states are direct generalizations of the Fermi HNC equations in II. The chain  $G_{xx',mn}$  classified according to the type of exchanges  $xx'$  at its ends  $m$  and  $n$ . The classifications having  $xx' = dd, de, ee,$  and  $cc$ , which, respectively, describe chains with both ends direct, one direct one exchange, both exchange, and those having an incomplete  $l$  loop passing through both ends, are sufficient to describe all the chains in Fermi systems. Two more types of chain functions are needed to sum many-body  $p$  loops in the present case. These have  $xx' = vv$  and  $pp$ ; the  $G_{vv,mn}$  is defined as the sum of all chains having an incomplete loop made up of  $\hat{l}$  lines, while  $G_{pp,mn}$  is the sum of chains having an incomplete loop of one  $p$  line and any number of  $\hat{l}$  lines.

We define

$$Z_{xx'} = G_{xx'} + C_{xx'} + E_{xx'} \quad (3.1)$$

where  $C_{xx',mn}$  denotes the sum of diagrams of type  $xx'$  having  $f_{3,mn}^2 - 1$ , and  $E_{xx'}$  is the sum of the elementary diagrams. The functions  $L$ ,  $Q$ , and  $P$  that include many-body exchanges are then given by

$$L = l + Z_{cc} \quad , \quad (3.2)$$

$$Q = \hat{l} + Z_{vv} \quad , \quad (3.3)$$

$$P = p + Z_{pp} \quad . \quad (3.4)$$

The partial distribution functions are obtained as

$$g_{dd} = f_j^2 \exp(Z_{dd}) \quad , \quad (3.5)$$

$$g_{de} = g_{dd} Z_{de} \quad , \quad (3.6)$$

$$g_{ee} = g_{dd} (D + L^2 + 2QP + Z_{ee} + Z_{de}^2) \equiv g_{dd} M \quad , \quad (3.7)$$

$$g_{cc} = g_{dd} L \quad , \quad (3.8)$$

$$g_{vv} = g_{dd} Q \quad , \quad (3.9)$$

$$g_{pp} = g_{dd} P \quad , \quad (3.10)$$

and the total  $g$  is given by

$$g = g_{dd} + 2g_{de} + g_{ee} \quad . \quad (3.11)$$

The sum of non-nodal diagrams, which can be the links of the chains  $G_{xx',mn}$  is defined as  $X_{xx'}$ . We have

$$X_{dd} = g_{dd} - 1 - G_{dd} \quad , \quad (3.12)$$

$$X_{de} = g_{de} - G_{de} \quad , \quad (3.13)$$

$$X_{ee} = g_{ee} - G_{ee} \quad , \quad (3.14)$$

$$X_{cc} = g_{cc} - l - G_{cc} \quad , \quad (3.15)$$

$$X_{vv} = g_{vv} - \hat{l} - G_{vv} \quad , \quad (3.16)$$

$$X_{pp} = g_{pp} - p - G_{pp} \quad . \quad (3.17)$$

It is convenient to define the functions

$$Y_{xx'} = g_{xx'} - \delta_{xd} \delta_{x'd} \quad , \quad (3.18)$$

which for  $xx = dd$ ,  $de$ , and  $ee$  correspond to the sum of links and chains, while for  $xx = cc$ ,  $vv$ , and  $pp$  they give the sum of links, chains and the  $l$ ,  $\hat{l}$ , or  $p$ . The chain equations can then be written as

$$G_{xx',mn} = \sum_{ep} \rho \int d^3 r_1 X_{xy,m1} Y_{y'x',1n} \quad . \quad (3.19)$$

The  $\sum_{ep}$  is a sum over all allowed exchange patterns at node 1. These correspond to  $yy' = dd$ ,  $de$ ,  $ed$ ,  $cc$ ,  $vv$ ,  $vp$ , and  $p v$ . The Eq. (3.19) is very symbolic, particularly when  $xx'$  equal  $vp$  and  $p v$  they are to be understood as  $pp$ . There are no  $G_{vp}$  and  $G_{pv}$  functions; " $vp$ " and " $p v$ " chains are  $pp$  chains by definition.

The  $C_{xx}$  are given by

$$C_{dd} = \Gamma((1 + Z_{de}); 1) \quad , \quad (3.20)$$

$$C_{de} = \Gamma(1; (M + Z_{de})) + \Gamma(Z_{de}; Z_{de}) \quad , \quad (3.21)$$

$$C_{ee} = \Gamma(Z_{ed}; (2M + Z_{de})) \quad , \quad (3.22)$$

$$C_{cc} = \Gamma(L; L) \quad , \quad (3.23)$$

$$C_{vv} = \Gamma(Q; Q) \quad , \quad (3.24)$$

$$C_{pp} = \Gamma(2Q; P) \quad , \quad (3.25)$$

where  $\Gamma_{mn}(A; B)$  for any functions  $A_{ij}$ ,  $B_{ij}$  of  $r_{ij}$  is defined as

$$\Gamma_{mn}(A; B) = \rho \int d^3 r_1 g_{dd,m1} g_{dd,n1} (f_{3,mn}^2 - 1) A_{m1} B_{n1} \quad . \quad (3.26)$$

The  $D_{mn}$  is defined as the sum of all connected diagrams in which  $m$  and  $n$  are connected by either  $f_K$  lines or exchange lines connected to  $f_K$  lines. The  $D_{mn}$  diagrams having articulation points have to be treated with the general expansion (2.7). An expansion of  $D_{mn}$  into elementary clusters is given in II, and it may be used in the present case by simply letting each exchange loop be either an  $l$  loop or  $p$  loop.

The vertex correction function  $\hat{S}(k)$  required to compute the  $\hat{l}$  is given by

$$\hat{S}(\vec{k}) - 1 = \rho \int d^3 r_{ij} \exp(i\vec{k} \cdot \vec{r}_{ij}) (g_{dd,ij} - 1) P_{ij} \quad . \quad (3.27)$$

The  $\exp(i\vec{k} \cdot \vec{r}_{ij})$  in the above equation comes from the  $l_{ij}$  line, while  $(g_{dd,ij} - 1) P_{ij}$  is the sum of all diagrams that can complete the  $p$  loop.

The Eqs. (3.1)–(3.27) are so far exact; however, they include the infinite sums  $E_{xx'}$ , and  $D$  which cannot be exactly calculated. In the HNC approximation we neglect the  $E_{xx'}$ , which corresponds to neglect of the coupling between the  $G_{xx',ij}$ , the  $C_{xx',ij}$ , and that of  $G_{xx',ij}$  with  $C_{xx',ij}$ . It has been argued in I that the coupling between the  $G_{xx',ij}$ , and that between  $G_{xx',ij}$  is probably weak, while that between the  $C_{xx',ij}$  could significantly reduce the contribution of terms having  $(C_{xx',ij})^{n \geq 2}$ . Following these arguments we will neglect both the  $E_{xx'}$  and terms having  $(C_{xx',ij})^{n \geq 2}$ . Note that this still allows quadratic terms of type  $C_{xx',ij} C_{yy',jk}$ , etc., in the chains.

The integral equations given above can be easily modified to ignore  $(C_{xx',ij})^{n \geq 2}$  terms. We first define partial exchange functions  $\bar{L}_{mn}$ ,  $\bar{Q}_{mn}$ , and  $\bar{P}_{mn}$ , and partial distribution functions  $\bar{g}_{xx',mn}$  such that they do not have any contribution from  $C_{xx',mn}$ . These functions are obtained by replacing the  $Z_{xx'}$  in Eqs. (3.2)–(3.10) by  $G_{xx'}$ . The distribution functions that

contain at most linear terms in  $C_{xx',mn}$  are given by

$$g_{dd} = \bar{g}_{dd}(1 + C_{dd}) \quad , \quad (3.28)$$

$$g_{de} = \bar{g}_{dd}C_{de} + \bar{g}_{de}(1 + C_{dd}) \quad , \quad (3.29)$$

$$g_{ee} = \bar{g}_{dd}(C_{ee} + C_{de}G_{de} + 2LC_{cc} + 2QC_{pp} + 2C_{vv}P) \\ + \bar{g}_{ee}(1 + C_{dd}) \quad , \quad (3.30)$$

$$g_{xx} = \bar{g}_{dd}C_{xx} + \bar{g}_{xx}(1 + C_{dd}) \\ xx = cc, vv, \text{ and } pp \quad . \quad (3.31)$$

The links  $X_{xx',mn}$  calculated with these  $g_{xx'}$  do not have multiple  $C_{xx'}$ . The  $\hat{S}(k)$  Eq. (3.27) is modified to be

$$\hat{S}(\vec{k}) - 1 = \rho \int d^3r e^{i\vec{k}\cdot\vec{r}} [(g_{dd} - 1)\bar{P} + (\bar{g}_{dd} - 1)C_{pp}] \quad . \quad (3.32)$$

It is found in II that the dressed two-body clusters give the dominant contribution to  $D$  in liquid  $^3\text{He}$ ; thus only these are included in the present work. The calculation of their contribution in the Bose excited state is not much different from that in Fermi

liquids, and the  $D$  in this approximation is given by

$$D \approx 2 \frac{\eta r}{f_j} l'(P + L) + \left( \frac{\eta r}{f_j} \right)^2 \left[ \frac{\langle k^2 \rangle}{6} - \frac{l''}{2}(L + P) + l'^2 \right] \quad , \quad (3.33)$$

where  $l'$  and  $l''$  are the first and second derivatives of  $l(r)$ , and  $\langle k^2 \rangle$  is the average value of  $k^2$  in the  $\Phi(n(k))$

$$\langle k^2 \rangle = \frac{1}{A} \sum_{\vec{k}} k^2 n(\vec{k}) \quad . \quad (3.34)$$

Note that the uncorrected Slater function  $l$  has been used in Eq. (3.33) for the dressed two-body  $D$ . Vertex corrections to the dressed two-body  $D$  will be of the same order as many-body cluster contributions to  $D$ , and they should be taken together.

#### IV. CALCULATION OF $E(n(\vec{k}))$

The  $E(n(\vec{k}))$  contains the expectation value of the two-body interaction  $v_{mn}$ , and the kinetic energy. It is convenient to divide  $E(n(\vec{k}))$  into seven parts

$$E(n(\vec{k})) = W + U + T + W_F + U_F + T_F + S \quad , \quad (4.1)$$

of which only  $W$ ,  $U$ , and  $T$  contribute to the ground-state energy. They are given by

$$W = \frac{1}{2} \rho \int g(r) \left[ v(r) - \frac{\hbar^2}{m} (\nabla^2 f_j) / f_j \right] d^3r \quad , \quad (4.2)$$

$$U = \frac{\hbar^2}{2m} \rho^2 \int g_{3,mno} \frac{(\vec{\nabla}_m f_{J,mn}) \cdot (\vec{\nabla}_m f_{J,mo})}{f_{J,mn} f_{J,mo}} d^3r_{mn} d^3r_{mo} \quad , \quad (4.3)$$

$$T = - \frac{\hbar^2}{4m} \rho^2 \int \frac{g_{3,mno}}{f_{3,mno}} \left[ \nabla_m^2 f_{3,mno} + 2(\vec{\nabla}_m f_{3,mno}) \cdot \left( \frac{(\vec{\nabla}_m f_{J,mn})}{f_{J,mn}} + \frac{(\vec{\nabla}_m f_{J,mo})}{f_{J,mo}} \right) \right] d^3r_{mn} d^3r_{mo} \quad , \quad (4.4)$$

where  $g(r)$  is the two-particle distribution function [Eq. (3.11)], and the three-particle distribution function is defined as

$$g_{3,mno} = \sum_{ep} f_{3,mno}^2 \bar{g}_{xx',mn} \bar{g}_{yy',mo} \bar{g}_{zz',no} \quad . \quad (4.5)$$

The  $\sum_{ep}$  implies a sum over  $xx'$ ,  $yy'$ , and  $zz'$  that form allowed exchange patterns. Note that the  $T$  and  $U$  given above do not include terms of type  $\vec{\nabla}_m f_{3,mno} \cdot \vec{\nabla}_m f_{3,mpq}$  and  $\vec{\nabla}_m f_{3,mno} \cdot \vec{\nabla}_m f_{J,mp}$ . It has been argued in I that these terms should be treated along with their HNC/4 counterparts.

The  $T_F$  is the kinetic energy associated with the  $\Phi(n(\vec{k}))$ , and it is given exactly by

$$T_F = (\hbar^2/2m) \langle k^2 \rangle \quad . \quad (4.6)$$

The  $W_F$  and  $U_F$  give kinetic-energy contributions associated with

$$\vec{\nabla}_m (f_{J,mn} f_{3,mno}) \cdot \vec{\nabla}_m \Phi(n(\vec{k}))$$

terms

$$W_F = - \frac{\hbar^2}{m} \rho^2 \int \frac{(\vec{\nabla}_m f_{J,mn})}{f_{J,mn}} \cdot [g_{cc,mn} (\vec{\nabla}_m l_{mn}) + g_{pp,mn} (\vec{\nabla}_m \hat{l}_{mn})] d^3r_{mn} \quad , \quad (4.7)$$

$$U_F = - \frac{\hbar^2}{m} \rho^2 \int f_{3,mno}^2 \left[ \frac{(\vec{\nabla}_m f_{3,mno})}{f_{3,mno}} + \frac{(\vec{\nabla}_m f_{J,mn})}{f_{J,mn}} \right] \\ \cdot \{ [\bar{g}_{cc,mo} (\vec{\nabla}_m l_{mo}) + \bar{g}_{pp,mo} (\vec{\nabla}_m \hat{l}_{mo})] [\bar{g}_{dd,mn} (\bar{g}_{dd,on} + \bar{g}_{de,on}) + \bar{g}_{de,mn} \bar{g}_{dd,on}] \\ + (\vec{\nabla}_m l_{mo}) \bar{g}_{dd,mo} \bar{g}_{cc,on} \bar{g}_{cc,nm} + (\vec{\nabla}_m \hat{l}_{mo}) g_{dd,mo} (\bar{g}_{vv,on} \bar{g}_{pp,nm} + \bar{g}_{pp,on} \bar{g}_{vv,nm}) \} d^3r_{mn} d^3r_{mo} \quad (4.8)$$

Note that the  $U_F$  and  $W_F$  do not contain contributions for diagrams having  $f_{K,mn}$  or  $f_{K,mo}$ . These are included along with terms of type  $\nabla_m^2 f_{K,mn}$  and  $\bar{\nabla}_m f_{K,mn} \cdot \bar{\nabla}_m \Phi$  in the  $S$ .

The expansion of  $S$  is discussed in II. We include only the dressed two-body diagrams that contribute to  $S$ . Their contribution is calculated, as in II, by defining

$$q = \eta/f_J \quad , \quad (4.9)$$

$$t_{mn} = \frac{f'_{J,mn}}{f_{J,mn}} + \rho \int d^3r_0 \left[ \bar{g}_{dd,mo} \bar{g}_{dd,on} + \bar{g}_{dd,mo} \bar{g}_{ed,on} + \bar{g}_{de,mo} \bar{g}_{dd,on} \right] f_{3,mno} \frac{1}{f_{J,mo}} [\hat{r}_{mn} \cdot (\bar{\nabla}_m f_{3,mno} f_{J,mo})] \quad , \quad (4.10)$$

$$s = \frac{1}{2} (q''r + 4q') + (q'r + q)t \quad . \quad (4.11)$$

The  $S$  is given by

$$-\frac{\hbar^2}{2m} \rho \int d^3r g_{dd} \{ -\langle k^2 \rangle (q'r + 3q) + 2sl'(L+P) + (2qrt + q'r + q)[l''(L+P) + l'^2] + (2q/r)l'(L+P) \\ + \frac{1}{2} (qrt + q'r + q)qr[l'''(L+P) + 3l''l'] + q^2[(l'' - l'/r)(L+P) + l'^2] \} \quad . \quad (4.12)$$

When  $n(k > 0) = 0$  the  $\langle k^2 \rangle$ ,  $l$ , and  $\hat{l}$  are all zero and the  $W_F$ ,  $U_F$ ,  $T_F$ , and  $S$  vanish. The  $W$ ,  $U$ , and  $T$  depend upon the  $n(\bar{k})$  through the distribution functions  $g$  and  $g_{3,mno}$ . However, as stated in the Introduction, if  $\prod_{i < j} f_{J,ij} \prod_{i < j < k} f_{3,ijk}$  is close to an eigenfunction of  $H$  the  $W + U + T$  should be independent of  $n(\bar{k})$  and equal to  $E_0$  the ground-state energy.

## V. PHONON-ROTON SPECTRUM

The one-quasiparticle excitation spectrum  $\epsilon(K)$  is calculated by promoting a small fraction  $\alpha$  of the particles to the quasiparticle state  $\bar{K}$

$$n(\bar{k}) = \begin{cases} \alpha A, & \bar{k} = \bar{K} \\ (1 - \alpha)A, & \bar{k} = 0 \\ 0, & \bar{k} \neq \bar{K}, 0 \end{cases} \quad (5.1)$$

$$(1 - \alpha)A, \quad \bar{k} = 0 \quad (5.2)$$

$$0, \quad \bar{k} \neq \bar{K}, 0 \quad (5.3)$$

The  $E(n(\bar{k}))$  will then be a function of  $\alpha$  and  $K$ , and

$$\epsilon_1(K) = \lim_{\alpha \rightarrow 0} \frac{E(\alpha, K) - E_0}{\alpha} \quad . \quad (5.4)$$

If we assume that the  $\Psi_0$  given by the  $\mathcal{G}$  is the exact  $\hat{\Psi}_0$  we obtain

$$\epsilon_2(K) = \lim_{\alpha \rightarrow 0} [T_F(\alpha, K) + W_F(\alpha, K) \\ + U_F(\alpha, K) + S(\alpha, K)]/\alpha \quad . \quad (5.5)$$

The two equations (5.4) and (5.5) will generally not yield the same  $\epsilon(K)$ ; if the difference is large, Eq. (5.5) should not be used. We will calculate  $\epsilon(K)$  with both forms and use the difference between them as an estimate of the quality of our  $\mathcal{G}$ .

Before discussing the present calculation of  $\epsilon(K)$  it

is instructive to verify the Feynman phonon spectrum with Eq. (5.5). The Feynman phonon spectrum<sup>10</sup> at small  $K$  is given by

$$\epsilon(K \rightarrow 0) = \frac{\hbar^2 K^2}{2mS(K)} \quad , \quad (5.6)$$

where  $S(K)$  is the static structure function for the ground state

$$S(K) = 1 + \rho \int (g(\bar{r}) - 1) \exp(i\bar{K} \cdot \bar{r}) d^3r \quad .$$

The  $S(K)$  is linear in  $K$  at small  $K$ , and so is the  $\epsilon(K)$ .

It may be verified that the  $f_K$  contribution to the wave function is proportional to  $K^2$  at small  $K$ , and thus negligible. The two terms in  $\Phi(n(k))$  on which the  $\bar{\nabla}_{ij}$  in  $f_{K,ij}$  can operate to give a correlation are  $\exp(i\bar{K} \cdot \bar{r}_i)$  and  $\exp(i\bar{K} \cdot r_j)$ . Their sum can be written in relative ( $\bar{r}_{ij}$ ) and center-of-mass ( $\bar{R}_{ij}$ ) coordinates as

$$\exp(i\bar{K} \cdot \bar{r}_i) + \exp(i\bar{K} \cdot \bar{r}_j) \\ = \exp(i\bar{K} \cdot \bar{R}_{ij}) [\exp(i\frac{1}{2}\bar{K} \cdot \bar{r}_{ij}) + \exp(-i\frac{1}{2}\bar{K} \cdot \bar{r}_{ij})] \quad . \quad (5.7)$$

The  $\bar{\nabla}_{ij}$  operating on the relative wave function can only give terms having  $K^2$  and higher powers of  $K$ .

Thus, the phonon spectrum at small  $K$  is given by Eq. (5.5) with  $S(\alpha, K) = 0$ . The  $T_F(\alpha, K)$  is obviously  $(\hbar^2/2m)K^2\alpha$ , and we only need to calculate the terms in  $W_F$  and  $U_F$  that are linear in  $\alpha$ . These terms are given by diagrams that have a  $p$  loop with only one  $\hat{l}$  line. The  $\hat{S}(K)$  [Eq. (3.27)] is needed only in the limit  $\alpha \rightarrow 0$  where it becomes the structure function  $S(K)$ , and  $\hat{l}$  becomes

$$\hat{l} = \frac{\alpha e^{i\bar{K} \cdot \bar{r}}}{S(K)} \quad . \quad (5.8)$$

The sum of all  $W_F$  and  $U_F$  diagrams having only one

$\hat{l}$  line is given by

$$(W_F + U_F)_{\text{lin}} = -\frac{\hbar^2}{2m} \rho \alpha \int [\vec{\nabla} \hat{l}(r)] \cdot [\vec{\nabla} g(r)] d^3r$$

$$= -\frac{\hbar^2 K^2}{2m} \alpha \left( 1 - \frac{1}{S(K)} \right), \quad (5.9)$$

and inserting this in Eq. (5.5) gives the Feynman phonon spectrum.

We first discuss results of calculations in which  $f_{3,ijk}$  is set to unity, so that  $\mathcal{G}$  does not induce any three-body correlations. This corresponds to setting the variational parameter  $\beta_3$  in  $\mathcal{G}$  to zero. The  $\mathcal{G}$  then has only one variational parameter  $d$  which is varied to minimize  $E_0$  the ground-state energy. Its value is generally close to  $2r_0$ .

The  $\epsilon_1(K)$  and  $\epsilon_2(K)$  calculated from the equations (5.4) and (5.5) with  $\mathcal{G}(d=2r_0, \beta_3=0)$  at  $\rho=0.365 \sigma^{-3}$ , the experimental equilibrium density, are shown in Fig. 4. The results of Feynman and Cohen<sup>1</sup> (FC), and the experimental spectrum<sup>11</sup> are also shown for comparison.

In the phonon region ( $K < 2 \sigma^{-1}$ ) the  $\epsilon_1(K)$  and  $\epsilon_2(K)$  are not very close, and they are not linear in  $K$  as they should be. This incorrect behavior of  $\epsilon_1(K)$  and  $\epsilon_2(K)$  at small  $K$  is definitely due to the wrong asymptotic behavior of the  $f_j(r \rightarrow \infty)$  in our  $\mathcal{G}$ . We have  $f_j(r > d) = 1$  instead of the correct behavior

$$f_j(r \rightarrow \infty) = 1 - \frac{mc}{2\hbar\rho\pi^2} \frac{1}{r^2}, \quad (5.10)$$

where  $c$  is the sound velocity. Consequently the calculated  $S(K)$  is not linear in  $K$  at small  $K$ , and the calculated vertex corrections  $1/S(K)$  are incorrect. We hope that this difficulty may be easily eliminated

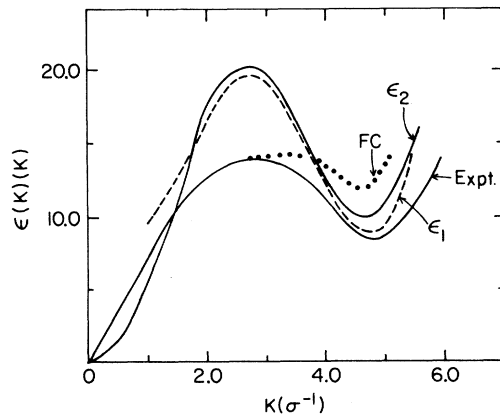


FIG. 4. The  $\epsilon_1(K)$  and  $\epsilon_2(K)$  calculated at  $\rho=0.365 \sigma^{-3}$ , and  $\beta_3=0$ , are compared with the spectra calculated by FC, and the experimental spectra.

by imposing the asymptotic behavior in Eq. (5.10) on the  $f_j$  in  $\mathcal{G}$ . FC use the experimental  $S(K)$  and get the exact  $E(K \rightarrow 0)$ .

The  $\epsilon_1(K)$  and  $\epsilon_2(K)$  are reasonably close (within about 0.5 K) in the region of maxon ( $2 < K < 4 \sigma^{-1}$ ), but our calculated maxon energies are much too large. The  $\epsilon(K)$  in this region should be sensitive to the tail of the back-flow correlation  $\eta_{ij}$ . The  $\eta_{ij}(r > d) = 0$  in our  $\mathcal{G}$ , but it should in fact<sup>1</sup> go as  $1/r^3$  as  $r \rightarrow \infty$ . FC assume  $(\eta/f_j) \propto 1/r^3$  and get this part of the spectrum correctly.

In the region of rotons ( $K \sim 5 \sigma^{-1}$ ) the  $\epsilon_1(K)$  and  $\epsilon_2(K)$  are in reasonable agreement with the experiment and each other. Here we do a little better than FC, hopefully because our  $\eta(r)$  at small  $r$  is better than that of FC.

The general character of  $\epsilon(K)$  does not change drastically when the three-body correlations are added to  $\mathcal{G}$ . The main effect, which can be seen from Table I, is that the  $\epsilon_1(K)$  and  $\epsilon_2(K)$  come much closer to each other, particularly in the maxon region. The  $\epsilon(K)$  in maxon region moves up away from the experimental results, while it moves down towards the experimental results in the roton region. Figures 5 and 6 show the experimental<sup>12</sup> and calculated roton energies at the experimentally observed densities under pressures of 1, 10, and 24 atm, respectively. The minimum values of  $E_0$  obtained at  $d=2r_0$ ,  $\beta_3=\beta_{3,\text{min}}$  are given in Table II. These  $E_0$  are almost identical to those reported in I.

The results obtained with  $\mathcal{G}(d=2r_0, \beta_3=0)$  are shown in Fig. 5, while those with  $\mathcal{G}(d=2r_0, \beta_3=\beta_{3,\text{min}})$  are in Fig. 6. The general density dependence of the roton energies seems to be well reproduced, particularly by the  $\mathcal{G}(d=2r_0, \beta_3=\beta_{3,\text{min}})$ . The

TABLE I. The one-quasiparticle excitation spectrum of liquid  $^4\text{He}$ .

$K (\sigma^{-1})$	$\epsilon_1(K, \beta_3=0)$	$\epsilon_2(K, \beta_3=0)$	$\epsilon_1(K, \beta_{3,\text{min}})$	$\epsilon_2(K, \beta_{3,\text{min}})$
1.0	9.02	5.53	13.49	12.34
1.5	12.57	11.20	15.77	15.68
2.0	15.52	16.87	17.33	17.50
2.5	18.94	19.76	20.87	20.84
3.0	19.09	19.68	22.49	22.62
3.5	16.52	16.90	18.90	19.00
4.0	12.67	12.82	12.41	12.68
4.5	9.16	9.99	8.38	9.11
5.0	8.92	10.35	9.34	10.07
5.5	13.76	14.53	15.00	15.08
6.0	23.15	22.12	24.18	23.24

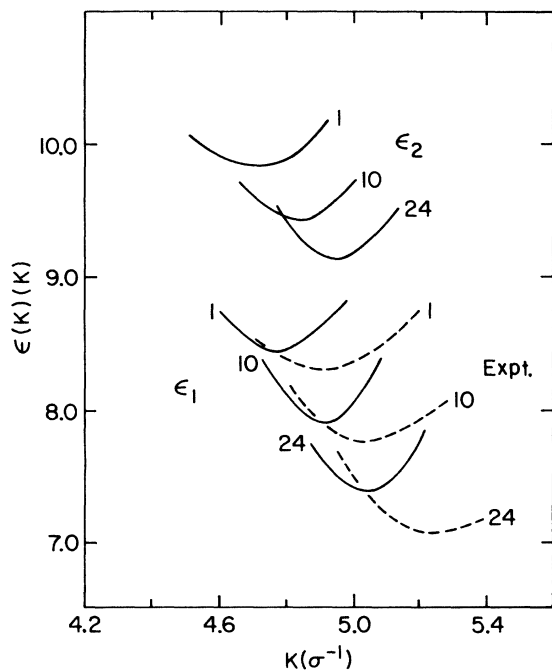


FIG. 5. The calculated roton energies at  $\rho = 0.367, 0.398$  and  $0.433 \sigma^{-3}$ , and  $\beta_3 = 0$ , are compared with the experimental values shown by broken lines. The curves are labeled with the experimental pressures (1, 10, and 24 atm) at these densities.

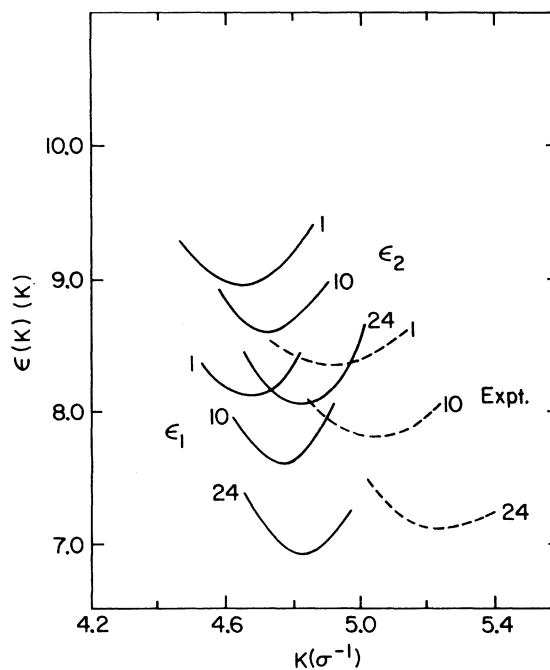


FIG. 6. The same as Fig. 5, except with  $\beta_3 = \beta_{3, \min}$ .

main problems appear to be (i) the minima in  $\epsilon(K)$  come at smaller values of  $K$ , and (ii) the curvature at the minima is much too large. The first of these could be related to the smallness of the core of the deBoer-Mitchels (6,12) potential. We also note that the  $\epsilon_2(K)$  is  $\sim 1$  K higher than  $\epsilon_1(K)$  even after including  $f_{3,ijk}$ ; without it the  $\epsilon_2(K)$  is  $\sim 2$  K above  $\epsilon_1(K)$ . As was noted earlier by Chang and Campbell,<sup>7</sup> there is a noticeable improvement in the densi-

ty dependence of roton energy on inclusion of  $f_{3,ijk}$ .

It thus appears that a microscopic realization of the correspondence between low-lying states of interacting and noninteracting quantum fluids may be possible via a reasonably simple correlation operator  $\mathcal{G}$ . However, the large distance behavior of the Jastrow and the backflow correlations in the present  $\mathcal{G}$  needs to be improved, to obtain proper excitation spectra or finite-temperature properties.

TABLE II. The ground-state energy at  $d = 2r_0$ .

$\rho(\sigma^{-3})$	$P$ (atm)	Expt.		Calculated	
		$E_0$ (K)	$E_0(\beta_{3, \min})$	$\beta_{3, \min}$	$E_0(\beta_3 = 0)$
0.367	1	-7.14	-6.65	1.7	-5.57
0.398	10	-7.0	-6.64	1.8	-5.19
0.433	24	-6.6	-6.41	2.1	-4.46

## ACKNOWLEDGMENT

This work was supported by the NSF PHY, Contract No. 78-26582.

---

\*Current address: Courant Institute of Mathematical Sciences, New York University, New York, N.Y. 10012.

<sup>1</sup>R. P. Feynman and M. Cohen, Phys. Rev. 102, 1189 (1956).

<sup>2</sup>V. R. Pandharipande, Phys. Rev. B 18, 218 (1978).

<sup>3</sup>K. E. Schmidt and V. R. Pandharipande, Phys. Rev. B 19, 2504 (1979).

<sup>4</sup>K. E. Schmidt and V. R. Pandharipande, Phys. Lett. B 87, 11 (1979).

<sup>5</sup>H. W. Jackson and E. Feenberg, Rev. Mod. Phys. 34, 686 (1962).

<sup>6</sup>T. C. Padmore and G. V. Chester, Phys. Rev. A 9, 1725 (1974).

<sup>7</sup>C. C. Chang and C. E. Campbell, Phys. Rev. B 13, 3779 (1976).

<sup>8</sup>J. deBoer and A. Michels, Physica (Utrecht) 5, 945 (1938).

<sup>9</sup>R. B. Wiringa and V. R. Pandharipande, Nucl. Phys. A 299, 1 (1978).

<sup>10</sup>R. P. Feynman, Phys. Rev. 94, 262 (1954).

<sup>11</sup>R. A. Cowley and A. D. B. Woods, Can. J. Phys. 49, 177 (1971).

<sup>12</sup>O. W. Dietrich, E. H. Graf, C. H. Huang, and L. Passell, Phys. Rev. A 5, 1377 (1972).